ELSEVIER

Available online at www.sciencedirect.com

SCIENCE DIRECT®

Nuclear Instruments and Methods in Physics Research B 216 (2004) 57–61

NIM B
Beam Interactions with Materials & Atoms

www.elsevier.com/locate/nimb

The laser annealing induced phase transition in silicon: a molecular dynamics study

Luis A. Marqués *, Lourdes Pelaz, María Aboy, Juan Barbolla

Departamento de Electricidad y Electrónica, Univesidad de Valladolid, E.T.S.I. de Telecomunicación, Campus Miguel Delibes s/n, 47011 Valladolid, Spain

Abstract

Laser thermal annealing of pre-amorphized silicon can be used to achieve sharp junctions with enhanced dopant activation. The changes in the properties of silicon as a consequence of the phase transition form amorphous to liquid caused by the laser annealing could influence the subsequent recrystallization and the activation of the dopants. In this work we have used the molecular dynamics simulation technique to study the physics of the amorphous-to-liquid transition in silicon. The changes in density, internal energy, structure and diffusion behavior are obtained from the simulations and analyzed. We have observed that for temperatures between the amorphous and crystal melting points there exists an intermediate phase which shares some of the properties of the amorphous and liquid silicon.
© 2003 Elsevier B.V. All rights reserved.

PACS: 61.72.Cc; 61.43.Dq; 61.82.Fk; 64.60.Cn
Keywords: Molecular dynamics; Silicon; Amorphous; Liquid; Phase transition

1. Introduction

To meet the semiconductor industry requirements about electronic devices under the 100 nm feature size, ultrashallow p^+/n junctions with active carrier concentrations above solubility limits will be required in the near future [1]. However, the widely used method to form shallow junctions, ion implantation followed by thermal annealing, shows several serious problems. In the particular case of boron, the impurity routinely used to form p-type zones in silicon, these are the channeling during implantation, and the transient enhanced diffusion and deactivation of the dopants during annealing [2].

In recent years, it has been demonstrated that ultrashallow box-like p^+/n junctions with high active concentrations can be formed by laser processing of pre-amorphized doped silicon [3]. These promising results suggest that this technique could be used in order to meet the industry downscaling requirements. In this process, the substrate is first bombarded by Ge or Si ions to form a shallow amorphous layer where the dopant is subsequently implanted. Then the sample surface is laser irradiated. It has been shown that when the laser pulse lasts longer than the electron–lattice relaxation time, direct transfer of energy from excited electrons to the lattice leads to thermal melting [4].

* Corresponding author. Tel.: +34-83-432000; fax: +34-983-423675.
E-mail address: lmarques@ele.uva.es (L.A. Marqués).

0168-583X/$ - see front matter © 2003 Elsevier B.V. All rights reserved.
doi:10.1016/j.nimb.2003.11.020

Since amorphous silicon melts 200 K below the melting point of crystal silicon [5], it is possible to set the laser power to just melt the shallow amorphous layer. This temperature window allows the epitaxial growth of the underlying crystal phase from the liquid–solid interface. The solidification occurs at a velocity of meters per second, several orders of magnitude higher than that found during conventional thermal treatments [4]. The dopant diffuses fast in the liquid phase and box-like profiles with concentrations above the solubility limits are obtained.

Depending on the laser irradiation parameters the regrown material can be perfect crystal, polycrystalline or even amorphous [4]. It has been shown that the laser fluence and the thermal properties of the material play an important and interdependent role, since the heat flow following the laser energy deposition determines the sample temperature as a function of time and space. For high undercoolings stacking faults and eventually amorphous layers can be formed instead of having perfect crystal regrowth, which can negatively influence the activation of the dopants and thus the device characteristics [6].

In this work we have used the molecular dynamics simulation technique to study the change of the properties and structure of amorphous silicon as a function of temperature, in order to get an atomistic picture of what happens during the laser annealing treatment. In Section 2 we introduce briefly the molecular dynamics technique as well as the conditions in which we have carried out our simulations. In Section 3 we present the results we have obtained regarding different properties of the amorphous phase, as well as its recrystallization behavior. Finally, we give some conclusions in Section 4.

2. Molecular dynamics simulations

The molecular dynamics technique consists of the computer-assisted resolution of the equations of motion for a set of N particles which constitute the system under study. From the time evolution of the positions, velocities and energies of the particles it is possible to extract meaningful physical properties, which in some cases can be directly compared with experiments, as well as to have a detailed picture of what is happening in the atomistic level [7].

The most important element in a molecular dynamics simulation is the definition of the forces, because they determine the system dynamics. In our case, to describe the silicon interactions we have used the empirical interatomic potential developed by Tersoff within its third parametrization (Tersoff 3), which has been shown to reproduce fairly well the different structures in which this element can appear (diatomic molecule, diamond, graphite, etc.) [8]. This potential includes an effective coordination term which is a function of bond lengths and their relative orientations, so the strength of a given bond depends on the coordination of the atoms that form it. In this way, the Tersoff potential appears to be adequate to describe phases of silicon where atoms are not perfectly fourfold coordinated, as it happens in amorphous and liquid silicon [9,10]. Unfortunately, the Tersoff 3 potential predicts a melting point for silicon around 2400 K [11], well above the experimental value of 1685 K. However, this is not a big drawback since it is possible to make a re-scaling between Tersoff temperatures and real temperatures [12].

Equations of motion were integrated using the fourth order Gear predictor-corrector algorithm [13] with a variable timestep depending on temperature, but always below 1 fs. All our simulations have been carried out at constant temperature by re-scaling atom velocities each 1000 timesteps. We have generated the amorphous phase by the accumulation of bond defects. The bond defect consists of a local rearrangement of bonds with no excess or deficit of atoms [14]. We have demonstrated in a previous paper that when introducing a concentration of bond defects above 30% in a perfect silicon lattice, homogeneous amorphization takes place [11]. We showed as well that the structure of the obtained amorphous matrix is in very good agreement with that corresponding to an amorphous sample obtained by slowly cooling from the melt.

We have carried out simulations using a silicon sample consisting of 1728 atoms in a computa-

tional cell whose dimensions were $12a \times 6\sqrt{2}a \times 6\sqrt{2}a$, a being the basic unit cell length (5.43 Å). Two-thirds of the sample (atoms with X coordinate above $4a$) were amorphized by introducing a concentration of 30% of bond defects. To minimize finite size effects, we used periodic boundary conditions along Y and Z axes, but not in the X axis. The two layers in the bottom of the crystal were held fixed to perfect lattice positions, and the amorphous surface was free to move. In this way the amorphous phase can accommodate any change on its density as a consequence of temperature fluctuations, which means that our simulations are also constant pressure. With this type of samples it is possible to extract some useful information regarding the amorphous phase and simultaneously study the recrystallization behavior from the amorphous–crystal interface.

3. Results and discussion

We have carried out simulations at different temperatures, starting from 1000 K and slowly heating up to 3000 K. By monitoring the evolution of the properties of atoms belonging to the amorphous part of the sample it is possible to characterize this phase as a function of temperature. In Fig. 1 we show the mean atomic potential energy evolution. For the sake of comparison, the potential energy corresponding to the crystal is also shown. The energy content of the amorphous is higher than in the case of crystal for all temperatures. As can be seen, it is possible to distinguish three temperature intervals: between 1000 and 1700 K the potential energy varies linearly, between 1700 and 2400 K its behavior its superlinear, and linear again between 2400 and 3000 K. Above 2400 K the potential energy values coincide with that corresponding with the liquid phase of silicon. In Fig. 2 we show the evolution of the density of the amorphous and crystal phases with temperature. For low temperatures the amorphous density is lower than the crystal density, in agreement with experiments, and in both cases it decreases with temperature. However, between 1500 and 2600 K, the amorphous density shows an anomalous behavior. It increases with temperature, surpassing the crystal value at around 1800 K. From 2600 K, the density again decreases. It is interesting to note that in this case the temperature intervals are not the same as in the previous one with the potential energies.

To analyze the structure of each sample we calculated the pair distribution functions. These are represented for several temperatures in Fig. 3. At 1000 K this function is the typical for an amorphous structure, with a clear first neighbor peak at a distance equal to the first neighbor distance in the crystal. There is a second peak at

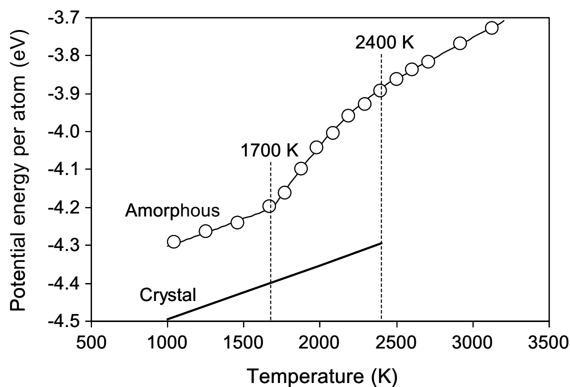

Fig. 1. Potential energy per atom in the amorphous and crystal phases of silicon as a function of temperature. Dotted lines show the temperatures where the potential energy of atoms belonging to the amorphous phase changes its behavior.

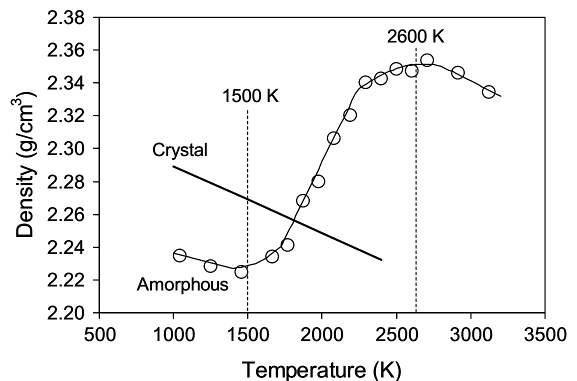

Fig. 2. Temperature evolution of the density of the amorphous and crystal phases of silicon. Dotted lines delimit the temperature interval where the amorphous phase shows an anomalous behavior.

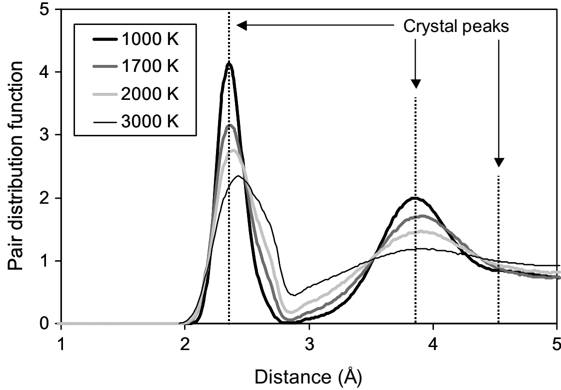

Fig. 3. Pair distribution function for the amorphous phase at different temperatures. The shape of the function changes gradually from the one typical of an amorphous solid to that of a liquid as temperature is increased. Dotted lines show the positions of the crystal peaks corresponding to the first, second and third neighbor shells.

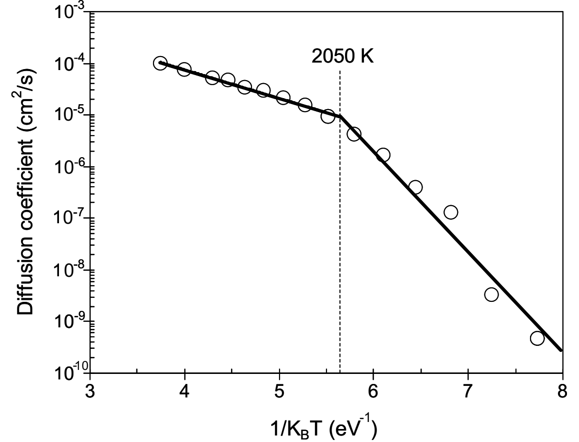

Fig. 4. Arrhenius plot of the diffusion coefficients for the amorphous phase. At a temperature of 2050 K there is a change in the diffusion behavior, which we attribute to the amorphous-to-liquid transition in the Tersoff 3 model of silicon. Below and above this temperature, data points have been fitted to exponential functions, shown in the figure as solid lines.

the second neighbor distance. As temperature is increased, the two peaks broaden, merge and their heights diminish, showing the typical structure of a liquid.

So it is clear that for temperatures below 1500 K the structure is that corresponding to an amorphous solid, and above 2400 K to a liquid. The transformation from amorphous to liquid with increasing temperature appears to be smooth and gradual. The exact transition temperature can be determined by inspection of the atomic movement. It is possible to calculate the atomic diffusion coefficients D at every temperature from the mean atomic displacements by applying the Einstein formula:

$$D = \frac{1}{6t}\sum_{i=1}^{N}|\vec{r}_i(t) - \vec{r}_i(0)|^2, \qquad (1)$$

which is valid for large enough values of time t. The diffusion coefficients are represented in the Arrhenius plot of Fig. 4. We can see a clear change in the diffusion behavior at around 2050 K. Above this temperature, diffusion coefficients are of the order of 10^{-4} cm^2/s, in agreement with ab initio simulations of the liquid silicon diffusion [15], and below they drop abruptly. We have also observed a different behavior regarding the recrystallization from the crystal-amorphous interface. In all the simulations carried out at temperatures equal to 2100 K and above, perfect recrystallization takes place. On the contrary, below 2100 K recrystallization shows frequent twining and stacking sequence defects. We believe these changes in the diffusion and recrystallization behaviors are produced because at 2050 K the amorphous-to-liquid transition takes place in the Tersoff 3 model of silicon. The drop in the diffusion coefficients indicate a viscosity increase below 2050 K. Atoms in the amorphous-crystal interface that are in local potential energy minima but not consistent with perfect diamond lattice positions have not enough kinetic energy to overcome the potential well. This frozen atoms produce mismatches in the stacking sequence during the subsequent recrystallization.

4. Conclusions

We have carried out molecular dynamics simulations to study the changes in the physical properties and crystallization behavior of amorphous silicon under laser annealing. We have shown that for the temperature range analyzed,

the physical properties and structure of the amorphous phase in the Tersoff model of silicon change gradually from the typical of a solid to that of a liquid. The transition to liquid takes place at 2050 K, a temperature 15% lower than the crystal melting point (2400 K) as in real silicon. Below this temperature, recrystallization shows frequent stacking faults along the amorphous-crystal interface produced by atoms trapped in local energy minima which are not consistent with the growing crystal. Above this temperature, these defects anneal out and recrystallization is perfect. More intensive investigation to further understand the nature of this transition is currently under way.

References

[1] The International Technology Roadmap for Semiconductors (International Sematech, Austin, Texas, 2001).

[2] E. Chason, S.T. Picraux, J.M. Poate, M.I. Current, T. Díaz de la Rubia, D.J. Eaglesham, O.W. Holland, M.E. Law, C.W. Magee, J.W. Mayer, J. Melngaillis, A.F. Tash, J. Appl. Phys. 81 (1997) 6513.

[3] Y.F. Chong, K.L. Pey, A.T.S. Wee, A. See, L. Chan, Y.F. Lu, W.D. Song, L.H. Chua, Appl. Phys. Lett. 76 (2000) 3197.

[4] P. Baeri, E. Rimini, Mater. Chem. Phys. 46 (1996) 169.

[5] E.P. Donovan, F. Spaepen, D. Turnbull, J.M. Poate, D.C. Jacobson, J. Appl. Phys. 57 (1985) 1795.

[6] A.G. Cullis, Mater. Res. Soc. Symp. Proc. 35 (1985) 15.

[7] M.P. Allen, D.J. Tieldesley, Computer Simulations of Liquids, Clarendon Press, 1994.

[8] J. Tersoff, Phys. Rev. B 38 (1988) 9902.

[9] M. Ishimaru, S. Munetoh, T. Motooka, K. Moriguchi, A. Shintani, Phys. Rev. B 58 (1998) 12583.

[10] J.K. Bording, J. Taftø, Phys. Rev. B 62 (2000) 8098.

[11] L.A. Marqués, L. Pelaz, J. Hernández, J. Barbolla, G.H. Gilmer, Phys. Rev. B 64 (2001) 045214.

[12] L.J. Porter, S. Yip, M. Yamaguchi, H. Kaburaki, M. Tang, J. Appl. Phys. 81 (1997) 96.

[13] C.W. Gear, Numerical Initial Value Problems in Ordinary Differential Equations, Prentice-Hall, 1971.

[14] M. Tang, L. Colombo, J. Zhu, T. Díaz de la Rubia, Phys. Rev. B 55 (1997) 14279.

[15] J.R. Chelikowsky, N. Troullier, N. Binggeli, Phys. Rev. B 49 (1994) 114.